JOURNAL OF AGRICULTURAL AND FOOD CHEMISTRY
ARTICLE

J. Agric. Food Chem. 2010, 58, 2643–2651 2643
DOI:10.1021/jf9026298

Design, Synthesis, and 3D-QSAR Analysis of Novel 1,3,4-Oxadiazol-2(3*H*)-ones as Protoporphyrinogen Oxidase Inhibitors†

Li-Li Jiang,[§,∥] Ying Tan,[§,#,∥] Xiao-Lei Zhu,[§] Zhi-Fang Wang,[§,#] Yang Zuo,[§] Qiong Chen,[§] Zhen Xi,*[,#] and Guang-Fu Yang*[,§]

[§] Key Laboratory of Pesticide and Chemical Biology of Ministry of Education, College of Chemistry, Central China Normal University, Wuhan 430079, People's Republic of China, and [#] State Key Laboratory of Elemento-Organic Chemistry, Nankai University, Tianjin 300071, People's Republic of China. [∥] Co-first authors.

Protoporphyrinogen oxidase (PPO, EC 1.3.3.4) has been identified as one of the most significant action targets for a large chemically diverse family of herbicides that exhibit some interesting characteristics, such as low use rate, low toxicity to mammals, and low environmental impact. As a continuation of research work on the development of new PPO inhibitors, some benzothiazole analogues of oxadiargyl, an important PPO-inhibiting commercial herbicide, were designed and synthesized by ring-closing of the substituents at the C-4 and C-5 positions. The bioassay results indicated that the series **8**, **9**, and **10** have good PPO inhibition activity with k_i values ranging from 0.25 to 18.63 μM. Most interestingly, **9l**, ethyl 2-((5-(5-*tert*-butyl-2-oxo-1,3,4-oxadiazol-2(3*H*)-yl)-6-fluorobenzothiazol-2-yl)sulfanyl) propanoate, was identified as the most promising candidate due to its high PPO inhibition effect (k_i = 1.42 μM) and broad spectrum postemergence herbicidal activity at the concentration of 37.5 g of ai/ha.

KEYWORDS: Protoporphyrinogen oxidase; 1,3,4-oxadiazol-2(3*H*)-ones; benzothiazole; herbicide

INTRODUCTION

As the last common enzyme in the biosynthesis pathway leading to heme and chlorophyll synthesis, protoporphyrinogen IX oxidase (PPO; EC 1.3.3.4) has been identified as one of the most significant targets for several chemical families of herbicides such as diphenyl ethers, phenylpyrazoles, oxadiazoles, triazolinones, thiadiazoles, pyrimidineones, oxazolidinediones, isoxazoles, and *N*-phenyl phthalimides that have been available in the commercial market for many years (*1*−*9*). It is well-known that the oxidation of protoporphyrinogen IX to protoporphyrin IX can take place nonenzymatically, but the PPO-catalyzed reaction seems to be ubiquitous in cells having aerobic metabolism (*9*, *10*). However, when the enzyme in plants is inhibited, the substrate protoporphyrinogen IX will accumulate and be exported to the cytoplasm, where it is slowly oxidized by O_2 to produce protoporphyrin IX (*11*). Then, when treated plants are exposed to visible radiation, the protoporphyrin IX, which is a highly efficient photosensitizer, will lead to severe photochemical damage, such as lipid peroxidation and cell death (*12*). Therefore, PPO-inhibiting herbicides are also known as light-dependent bleaching herbicides (*9*).

Most of side effects, such as toxicological and environmental impact, are associated with high use rates of herbicides (*13*). Therefore, PPO-inhibiting herbicides are of great interest due to their low use rates and environmentally benign characteristics. Since the 1970s, research on PPO inhibitors has been actively pursued, leading to two classes of commercial products, diphenyl ethers and *N*-phenyl phthalimides, the latter of which has become a very interesting research area (*13*−*16*). Structural optimization of the pioneering compounds of the *N*-phenyl phthalimides family, chlorphthalim and oxadiazon, as shown in **Figure 1**, resulted in the discovery of several commercial herbicides. Oxadiargyl, 3-[2,4-dichloro-5-(2-propynyloxy)phenyl]-5-(1,1-dimethylethyl)-1,3,4-oxadiazol-2-(3*H*)-one, is an oxadiazole-type PPO-inhibiting herbicide introduced in 1996. Although it exhibited some advantages over other PPO inhibitors, such as its broad spectrum, soil-independent, and low use rate properties, it is safe on crops only when applied as a pre-emergence herbicide (*14*−*16*). Therefore, it is an interesting task to discover new analogues with suitable postemergence herbicidal activity.

Oxadiazole-type herbicides have a common structural feature of *N*-2,4,5-trisubstituted phenylnitrogen. Of the phenyl substitution patterns investigated (*4*), the ones that led to the most active compounds were F or Cl at C-2 and Cl at C-4, whereas the groups at the C-5 position have an important effect not only on the activity but also on the crop selectivity. Keep in mind that the benzothiazole moiety is a common substructure in a large number of compounds with a wide range of biological activities (*17*−*21*); therefore, as a continuation of our research work on the development of new PPO inhibitors, we are very interested in the benzothiazole-type ring-closing analogues of oxadiargyl as shown in **Scheme 1**. Herein, we report the detailed syntheses

† Part of the ECUST-Qian Pesticide Cluster.

*Corresponding authors [(Z.X.) telephone/fax +86-22-23504782, e-mail zhenxie@nankai.edu.cn; (G.-F.Y.) telephone +86-27-67867800, fax +86-27-67867141, e-mail gfyang@mail.ccnu.edu.cn].

Published on Web 12/02/2009

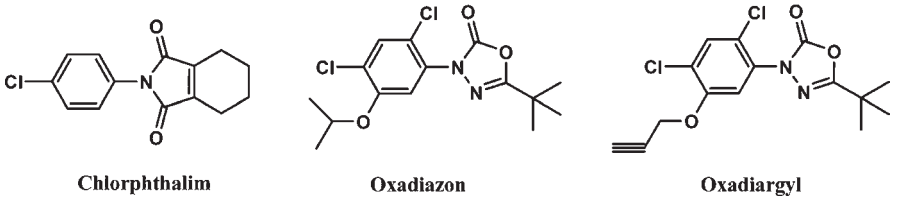

Figure 1. Structures of some commercial PPPO inhibitors.

Scheme 1. Molecular Design of the Series **8**, **9**, and **10**

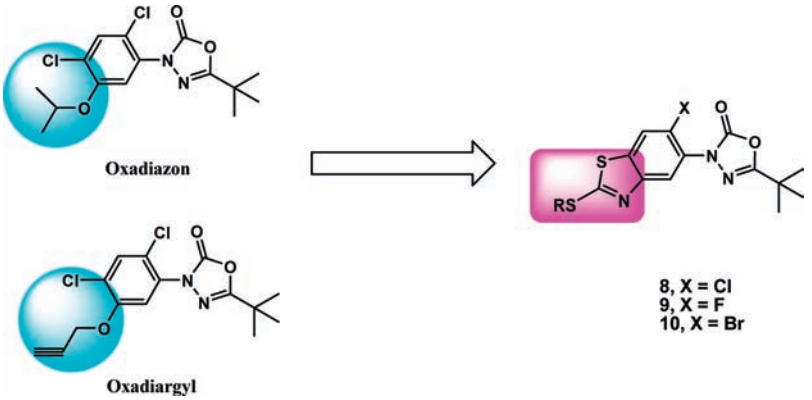

and herbicidal activities of series **8**, **9**, and **10**, and the results indicated that these compounds displayed good PPO inhibition activity and promising herbicidal activity.

MATERIALS AND METHODS

All chemical reagents were commercially available and treated with standard methods before use. Solvents were dried in a routine way and redistilled. ^{1}H NMR spectra were recorded on a Varian Mercury-Plus 400 spectrometer in $CDCl_3$ or DMSO-d_6 with TMS as the internal reference. Mass spectral data were obtained on a ThermoFisher Mass platform DSQII by electrospray ionization (ESI-MS). Elemental analyses were performed on a Vario EL III elemental analysis instrument. Melting points were taken on a Buchi B-545 melting point apparatus and uncorrected.

Preparation of (2,4-Disubstituted-phenyl)hydrazine Hydrochloride (2a−c) (*22*). Under a nitrogen atmosphere, a stirred solution of 2,4-dichloroaniline (**1a**, 4.80 g, 30 mmol) in 30 mL of concentrated hydrochloric acid was cooled to −9 °C, and a solution of 2.55 g (36 mmol) of sodium nitrite in 11 mL of water was added dropwise at a rate to keep the reaction mixture temperature under −9 °C. The complete addition required 20 min. The reaction mixture was stirred for an additional 1 h at 0 to −9 °C. Then, a solution of 14.8 g (78 mmol) of stannous chloride in 30 mL of concentrated hydrochloric acid was added dropwise at a rate to keep the reaction mixture temperature under −9 to −0 °C for 2 h. The mixture was then vacuum filtered, and the resulting solid was allowed to dry overnight. The solid was dissolved in hot water and gravity filtered, and the filtrate was cooled on ice. The crystallized solid was then suction filtered, and the product was allowed to dry overnight. **2a** was obtained as a solid in a yield of 39%, mp 191−193 °C (lit. (*23*) 193−194 °C). **2b** and **2c** were also prepared according to this procedure.

*Data for **2b**:* yield, 37%; mp, 209−210 °C; ^{1}H NMR (600 MHz, DMSO-d_6) δ 7.19−7.21 (m, 1H), 7.27−7.28 (m, 1H), 7.43−7.45 (m, 1H), 8.45 (br s, 1H), 10.38 (br s, 3H).

*Data for **2c**:* yield, 36%; mp, 208.0 °C (decomposition); ^{1}H NMR (600 MHz, DMSO-d_6) δ 7.15−7.17 (m, 1H), 7.29−7.32 (m, 1H), 7.58−7.59 (m, 1H), 7.89 (br s, 1H), 10.37 (br s, 3H).

Preparation of *N′*-(2,4-Disubstituted-phenyl)pivalohydrazide (3a−c) (*24*). A solution of sodium hydroxide (0.82 g, 20 mmol) in 20 mL of water was added dropwise to a stirred mixture of **2a−c** (13.8 mmol), 50 mL of H_2O, and 150 mL of CH_2Cl_2 in an ice bath. The reaction mixture was stirred for an additional 0.5 h. Then a solution of pivaloyl chloride (1.74 g, 14.5 mmol) in 20 mL of CH_2Cl_2 was added dropwise to the reaction system. After overnight stirring at room temperature, CH_2Cl_2 (100 mL) was added to the reaction mixture. The organic layer was separated and washed successively with water (200 mL) and brine (200 mL) and then dried over anhydrous magnesium sulfate. After evaporation of the solvent, the oil or solid products of **3a**, **3b**, and **3c** were obtained.

*Data for **3a**:* yield, 92%; yellow oil; ^{1}H NMR (400 MHz, $CDCl_3$) δ 1.29 (s, 9H), 6.73 (d, J = 8.4 Hz, 1H), 7.10 (dd, J_1 = 2.0 Hz, J_2 = 8.4 Hz, 1H), 7.29 (d, J = 2.0 Hz, 1H), 7.57 (br, 1H); ESI/MS, 260.0 (M^+).

*Data for **3b**:* yield, 93%; mp 135−137 °C; ^{1}H NMR (400 MHz, $CDCl_3$) δ 1.26 (s, 9H), 6.75 (t, J = 8.4 Hz, 1H), 6.98 (d, J = 8.4 Hz, 1H), 7.03 (d, J = 11.4 Hz, 1H), 7.57 (br, 1H); ESI/MS, 266.7 (M + Na).

*Data for **3c**:* yield, 86%; oil; ^{1}H NMR (400 MHz, $CDCl_3$) δ 1.28 (s, 9H), 6.75 (dd, J_1 = 5.2 Hz, J_2 = 8.8 Hz, 1H), 6.91−6.96 (m, 1H), 7.22 (dd, J_1 = 2.8 Hz, J_2 = 7.6 Hz, 1H); ESI/MS, 290.7 (M + H).

Preparation of 5-*tert*-Butyl-3-(2,4-disubstituted-phenyl)-1,3,4-oxadiazol-2(3*H*)-ones (4a−c) (*25*). Under a nitrogen atmosphere, a solution of bis(trichloromethyl) carbonate (7.46 g, 25.37 mmol) in toluene (50 mL) was added dropwise to a stirred solution of **3a−c** (12.69 mmol), triethylamine (2.57 g, 25.37 mmol), and toluene (260 mL) in an ice bath. The resulting mixture was stirred overnight at room temperature under a nitrogen atmosphere and then was refluxed for 2 h. After cooling, the solution was washed with water (200 mL) and brine (200 mL), then dried, filtered, and concentrated to give the desired oil or solid products.

*Data for **4a**:* yield, 90%; oil; ^{1}H NMR (400 MHz, $CDCl_3$) δ 1.37 (s, 9H), 7.35 (dd, J_1 = 2.4 Hz, J_2 = 8.4 Hz, 1H), 7.43 (d, J = 8.4 Hz, 1H), 7.54 (d, J = 2.0 Hz, 1H); ESI/MS, 286.1 (M).

*Data for **4b**:* yield, 90%; mp, 99−101 °C; ^{1}H NMR (400 MHz, $CDCl_3$) δ 1.37 (s, 9H), 7.25−7.28 (m, 2H), 7.46−7.50 (m, 1H); ESI/MS, 292.5 (M + Na).

*Data for **4c**:* yield, 92%; mp, 83−85 °C; ^{1}H NMR (400 MHz, $CDCl_3$) δ 1.37 (s, 9H), 7.15−7.16 (m, 1H), 7.45−7.51 (m, 2H); ESI-MS, 338.4 (M + Na).

Preparation of 5-*tert*-Butyl-3-(2,4-disubstituted-5-nitrophenyl)-1,3,4-oxadiazol-2(3*H*)-ones (5a−c). A solution of HNO_3 (1.07 g, 11.3 mmol) in concentrated H_2SO_4 (2.26 g, 22.6 mmol) was added dropwise to a stirred mixture of **4a−c** (11.3 mmol) and concentrated H_2SO_4 (226 mL) in an ice bath. The complete addition took about 15 min. After 3 h of stirring, the solution was slowly poured into a mixture of ice and water (500 mL). The resulting solid was collected by filtration, washed with water (2 L), and then dried to give to the desired solid products.

Data for ***5a****:* yield, 90%; mp, 155−156 °C; ^{1}H NMR (400 MHz, $CDCl_3$) δ 1.38 (s, 9H), 7.77 (s, 1H), 8.14 (s, 1H); ESI-MS, 331.9 (M + H).

Data for ***5b****:* yield, 83%; mp, 160−162 °C; ^{1}H NMR (400 MHz, $CDCl_3$) δ 1.38 (*s*, 9H), 7.47 (*d*, *J* = 9.6 Hz, 1H), 8.26 (*d*, *J* = 6.8 Hz, 1H); ESI-MS, 337.1 (M + Na).

Data for ***5c****:* yield, 87%; mp, 175−176 °C; ^{1}H NMR (400 MHz, $CDCl_3$) δ 1.39 (s, 9H), 7.70 (d, *J* = 9.6 Hz, 1H), 8.26 (d, *J* = 6.4 Hz, 1H); ESI-MS, 360.0 (M).

Preparation of 3-(5-Amino-2,4-disubstituted-phenyl)-5-*tert*-butyl-1,3,4-oxadiazol-2(3*H*)-ones (6a−c) (*26*). The powder of Fe was added portionwise to a stirred solution of NH_4Cl (0.83 g) and **5a−c** (10.4 mmol) in a mixture of EtOH/H_2O (v/v, 10:1, 220 mL) at reflux temperature. After TLC detection showing that the reaction had finished, the reaction mixture was filtered and concentrated to dryness. The residue was dissolved in water (200 mL) and extracted with EtOAc (200 mL); the organic phase was washed with brine (150 mL), dried, filtered, then concentrated to give the desired oil or solid products.

Data for ***6a****:* yield, 91%; oil; ^{1}H NMR (400 MHz, $CDCl_3$) δ 1.36 (s, 9H), 6.87 (s, 1H), 7.39 (s, 1H); ESI-MS, 301.6 (M).

Data for ***6b****:* yield, 69%; oil; ^{1}H NMR (600 MHz, $CDCl_3$) δ 1.36 (s, 9H), 3.90 (br, 2H), 6.90 (dd, J_1 = 7.2 Hz, J_2 = 1.2 Hz, 1H), 7.16 (dd, J_1 = 9.6 Hz, J_2 = 1.2 Hz, 1H); ESI-MS, 285.4 (M).

Data for ***6c****:* yield, 46%; mp, 122−124 °C; ^{1}H NMR (400 MHz, $CDCl_3$) δ 1.36 (s, 9H), 3.90 (br, 2H), 6.89 (d, *J* = 8.4 Hz, 1H), 7.28 (d, *J* = 10 Hz, 1H); ESI/MS, 329.3 (M).

Preparation of 5-*tert*-Butyl-3-(6-substituted-2-mercaptobenzo-[*d*]thiazol-5-yl)-1,3,4-oxadiazol-2(3*H*)-ones (7a−c) (*27*). A solution of **6a−c** (2.63 g, 9.45 mmol) and potassium *O*-ethyl dithiocarbonate (3.03 g, 18.9 mmol) in 142 mL anhydrous DMF was heated at 120 °C for 3 h. After TLC detection showing that the reaction had finished, the reaction mixture was evaporated under reduced pressure to remove most of the solvent and diluted with water (300 mL) and concentrated HCl solution until pH 3 to induce precipitation. Stirring was continued for 10 min. The solid precipitate was collected by filtration and rinsed with water. The wet filter cake was dried and then purified by flash column chromatography to give the pure products **7a**, **7b**, and **7c** in yields of 54, 60, and 53%, respectively.

Data for ***7a****:* mp, 155−156 °C; ^{1}H NMR (400 MHz, $CDCl_3$) δ 1.31 (s, 9H), 7.60 (s, 1H), 8.10 (s, 1H), 14.11 (s, 1H); ESI/MS, 341.9 (M + H).

Data for ***7b****:* mp, 158−160 °C; ^{1}H NMR (400 MHz, $CDCl_3$) δ 1.31 (s, 9H), 7.52 (d, *J* = 6.0 Hz, 1H), 7.91 (d, *J* = 9.6 Hz, 1H), 13.97 (s, 1H); ESI/MS, 387.3 (M + H).

Data for ***7c****:* mp, 150−152 °C; ^{1}H NMR (400 MHz, $CDCl_3$) δ 1.31 (s, 9H), 7.60 (s, 1H), 8.23 (s, 1H), 14.10 (s, 1H); ESI/MS, 337.9 (M + Na).

General Synthesis Procedure for the Target Series of 8, 9, and 10. K_2CO_3 powder (0.33 g, 2.4 mmol) was added to a solution of **7a**, **7b**, and **7c** (1.2 mmol) in acetone (20 mL). After 10 min of stirring at room temperature, halogen derivative (RX, 1.8 mmol) in acetone solution was added dropwise to the mixture. The resulting mixture reacted for about 30 min and then was filtered and concentrated. The residue was purified via flash chromatography to give the pure products **8**, **9**, and **10** in yields of 35−89%.

Data for ***8a****:* yield, 79%; mp 117−119 °C; ^{1}H NMR (400 MHz, $CDCl_3$) δ 1.39 (s, 9H), 4.09 (d, *J* = 7.6 Hz, 2H), 6.26 (t, *J* = 7.6 Hz, 1H), 7.90 (s, 1H), 7.98 (s, 1H); ESI-MS, 473.5 (M^+ + Na). Anal. Calcd for $C1_6H_{14}Cl_3N_3O_2S_2$.: C, 42.63; H, 3.13; N, 9.32. Found: C, 42.89; H, 3.23; N, 9.50.

Data for ***8b****:* yield, 35%; mp 160−161 °C; ^{1}H NMR (400 MHz, $CDCl_3$) δ 1.38−1.43 (m, 12H), 4.67 (q, *J* = 4.8 Hz, 2H), 8.04 (s, 1H), 8.10 (s, 1H); ESI-MS, 436.3 (M^+ + Na). Anal. Calcd for $C_{16}H_{16}ClN_3O_4S_2$: C, 46.43; H, 3.90; N, 10.15. Found: C, 46.20; H, 4.05; N, 10.04.

Data for ***8c****:* yield, 60%; mp 89−90 °C; ^{1}H NMR (400 MHz, $CDCl_3$) δ 1.26 (t, *J* = 7.2 Hz, 3H), 1.39 (s, 9H), 2.91 (t, *J* = 7.2 Hz, 2H), 3.61 (t, *J* = 7.2 Hz, 2H), 4.18 (q, *J* = 7.2 Hz, 2H), 7.89 (s, 1H), 7.96 (s, 1H); ESI-MS, 465.4 (M^+ + Na). Anal. Calcd for $C_{18}H_{20}ClN_3O_4S_2$: C, 48.92; H, 4.56; N, 9.51. Found: C, 48.68; H, 4.35; N, 9.62.

Data for ***8d****:* yield, 53%; mp, 98−100 °C; ^{1}H NMR (400 MHz, $CDCl_3$) δ 1.28 (t, *J* = 6.8 Hz, 3H), 1.39 (s, 9H), 4.17 (s, 2H), 4.24 (q, *J* = 6.8 Hz, 2H), 7.90 (s, 1H), 7.95 (s, 1H); ESI/MS, 427.2 (M^+). Anal. Calcd for $C_{17}H_{18}ClN_3O_4S_2$: C, 47.71; H, 4.24; N, 9.82. Found: C, 47.64; H, 4.44; N, 9.94.

Data for ***8e****:* yield, 46%; mp 142−143 °C; ^{1}H NMR (400 MHz, $CDCl_3$) δ1.40(*s*, 9H), 1.50(*s*, 9H), 4.08(*s*, 2H), 7.90(*s*, 1H), 7.94(*s*, 1H); ESI-MS, 477.1 (M^+ + Na). Anal. Calcd for $C_{19}H_{22}ClN_3O_4S_2$: C, 50.05; H, 4.86; N, 9.22. Found: C, 49.83; H, 4.76; N, 9.10.

Data for ***8f****:* yield, 72%; mp, 137−138 °C; ^{1}H NMR (400 MHz, $CDCl_3$) δ 1.39 (s, 9H), 3.80 (s, 3H), 4.18 (s, 2H), 7.90 (s, 1H), 7.97 (s, 1H); ESI-MS, 435.5 (M + Na). Anal. Calcd for $C_{16}H_{16}ClN_3O_4S_2$: C, 46.43; H, 3.90; N, 10.15. Found: C, 46.62; H, 4.10; N, 10.24.

Data for ***8g****:* yield, 61%; oil; ^{1}H NMR (400 MHz, $CDCl_3$) δ 1.25 (t, *J* = 7.2 Hz, 3H), 1.39 (s, 9H), 2.15 (m, 2H), 2.49 (t, *J* = 7.2 Hz, 2H), 3.41 (t, *J* = 7.2 Hz, 2H), 4.14 (q, *J* = 7.2 Hz, 2H), 7.89 (s, 1H), 7.95 (s, 1H); ESI-MS, 477.1 (M + Na). Anal. Calcd for $C_{19}H_{22}ClN_3O_4S_2$: C, 50.05; H, 4.86; N, 9.22. Found: C, 50.21; H, 4.62; N, 8.85.

Data for ***8h****:* yield, 59%; mp, 104−106 °C; ^{1}H NMR (400 MHz, $CDCl_3$) δ 1.25 (t, *J* = 7.2 Hz, 3H), 1.39 (s, 9H), 2.15 (d, *J* = 7.2 Hz, 3H), 4.22 (q, *J* = 7.2 Hz, 2H), 4.67 (q, *J* = 7.2 Hz, 1H), 7.90 (s, 1H), 7.96 (s, 1H); ESI/MS, 442.05 (M + H). Anal. Calcd for $C_{18}H_{20}ClN_3O_4S_2$: C, 48.92; H, 4.56; N, 9.51. Found: C, 49.13; H, 4.76; N, 9.60.

Data for ***8i****:* yield, 76%; mp, 116−117 °C; ^{1}H NMR (400 MHz, $CDCl_3$) δ 1.39 (s, 9H), 4.00 (d, *J* = 6.0 Hz, 2H), 5.22 (d, *J* = 10.0 Hz, 1H), 5.37 (d, *J* = 17.2 Hz, 1H), 5.96−6.03 (m, 1H), 7.89 (s, 1H), 7.97 (s, 1H); ESI/MS, 403.3 (M + Na). Anal. Calcd for $C_{16}H_{16}ClN_3O_2S_2$: C, 50.32; H, 4.22; N, 11.00. Found: C, 50.02; H, 4.44; N, 11.23.

Data for ***8j****:* yield, 80%; mp, 102−103 °C; ^{1}H NMR (600 MHz, $CDCl_3$) δ 1.20 (t, *J* = 7.2 Hz, 3H), 1.39 (s, 9H), 1.77 (s, 6H), 4.19 (q, *J* = 7.2 Hz, 2H), 7.91 (s, 1H), 7.99 (s, 1H); ESI/MS, 477.8 (M + Na). Anal. Calcd for $C_{19}H_{22}ClN_3O_4S_2$: C, 50.05; H, 4.86; N, 9.22. Found: C, 49.87; H, 4.63; N, 9.12.

Data for ***8k****:* yield, 69%; mp, 110.2−110.5 °C; ^{1}H NMR (600 MHz, $CDCl_3$) δ 1.26 (d, *J* = 9.6 Hz, 6H), 1.39 (s, 9H), 4.13 (s, 2H), 5.09 (m, 1H), 7.90 (s, 1H), 7.94 (s, 1H); ESI/MS, 463.0 (M + Na). Anal. Calcd for $C_{18}H_{20}ClN_3O_4S_2$: C, 48.92; H, 4.56; N, 9.51. Found: C, 49.13; H, 4.79; N, 9.60.

Data for ***8l****:* yield, 67%; mp, 88−89 °C; ^{1}H NMR (600 MHz, $CDCl_3$) δ 0.93 (t, *J* = 7.2 Hz, 3H), 1.39 (s, 9H), 1.67−1.68 (m, 2H), 4.14 (t, *J* = 6.0 Hz, 2H), 4.18 (s, 2H), 7.90 (s,1H), 7.95 (s,1H); ESI/MS, 463.0 (M + Na). Anal. Calcd for $C_{18}H_{20}ClN_3O_4S_2$: C, 48.92; H, 4.56; N, 9.51. Found: C, 48.65; H, 4.36; N, 9.44.

Data for ***8m****:* yield, 75%; mp, 96−98 °C; ^{1}H NMR (400 MHz, $CDCl_3$) δ 1.39 (s, 9H), 2.31 (t, *J* = 2.4 Hz, 1H), 4.14 (d, *J* = 2.4 Hz, 2H), 7.92 (s, 1H), 8.01 (s, 1H); ESI/MS, 401.8 (M + Na). Anal. Calcd for $C_{16}H_{14}ClN_3O_2S_2$: C, 50.59; H, 3.71; N, 11.06. Found: C, 50.67; H, 3.90; N, 11.23.

Data for ***9a****:* yield, 62%; mp, 113−114 °C; ^{1}H NMR (600 MHz, $CDCl_3$) δ 1.39 (s, 9H), 3.80 (s, 3H), 4.18 (s, 2H), 7.60 (d, *J* = 9.6 Hz, 1H), 8.13 (d, *J* = 4.2 Hz, 1H); ESI/MS, 398.03 (M + H). Anal. Calcd for $C_{16}H_{16}FN_3O_4S_2$: C, 48.35; H, 4.06; N, 10.57. Found: C, 48.57; H, 4.21; N, 10.70.

Data for ***9b****:* yield, 58%; mp, 143−144 °C; ^{1}H NMR (600 MHz, $CDCl_3$) δ 1.39 (s, 9H), 3.80 (s, 3H), 4.00 (s, 3H), 7.73 (d, *J* = 8.4 Hz, 1H), 8.13 (d, *J* = 6.6 Hz, 1H); ESI/MS, 383.2 (M^+). Anal. Calcd for $C_{15}H_{14}FN_3O_4S_2$: C, 46.99; H, 3.68; N, 10.96. Found: C, 47.18; H, 3.87; N, 11.14.

Data for ***9c****:* yield, 69%; mp, 151−152 °C; ^{1}H NMR (600 MHz, $CDCl_3$) δ 1.39 (s, 9H), 1.40 (t, *J* = 7.2 Hz, 3H), 4.46 (q, *J* = 7.2 Hz, 2H), 7.73 (d, *J* = 9.0 Hz, 1H), 8.0 (d, *J* = 6.6 Hz, 1H); ESI/MS, 419.6 (M + Na). Anal. Calcd for $C_{16}H_{16}FN_3O_4S_2$: C, 48.35; H, 4.06; N, 10.57. Found: C, 48.50; H, 4.28; N, 10.80.

Data for ***9d****:* yield, 67%; mp, 89−90 °C; ^{1}H NMR (600 MHz, $CDCl_3$) δ 1.28 (t, *J* = 7.2 Hz, 3H), 1.39 (s, 9H), 4.16 (s, 2H), 4.23 (q, *J* = 7.2 Hz, 2H), 7.60 (d, *J* = 9.6 Hz, 1H), 7.97 (d, *J* = 6.6 Hz, 1H); ESI/MS, 433.7 (M + Na). Anal. Calcd for $C_{17}H_{18}FN_3O_4S_2$: C, 49.62; H, 4.41; N, 10.21. Found: C, 49.40; H, 4.28; N, 10.10.

Data for ***9e****:* yield, 80%; mp, 143−145 °C; ^{1}H NMR (600 MHz, $CDCl_3$) δ 1.39 (s, 9H), 1.48 (s, 9H), 4.07 (s, 2H), 7.60 (d, *J* = 9.0 Hz, 1H), 8.0 (d, *J* = 6.0 Hz, 1H); ESI/MS, 460.4 (M + Na). Anal. Calcd for $C_{19}H_{22}FN_3O_4S_2$: C, 51.92; H, 5.05; N, 9.56. Found: C, 52.03; H, 5.25; N, 9.67.

Data for ***9f****:* yield, 84%; oil; ^{1}H NMR (600 MHz, $CDCl_3$) δ 1.39 (s, 9H), 3.99 (d, *J* = 7.2 Hz, 2H), 5.21 (d, *J* = 10.2 Hz, 1H), 5.37 (d, *J* = 16.8 Hz, 1H), 6.01−6.02 (m, 1H), 7.59 (d, *J* = 9.0 Hz, 1H), 7.98 (d, *J* = 6.6 Hz, 1H); ESI/MS, 387.5 (M + Na). Anal. Calcd for $C_{16}H_{16}FN_3O_2S_2$: C, 52.59; H, 4.41; N, 11.50. Found: C, 52.44; H, 4.11; N, 11.26.

Data for ***9g****:* yield, 61%; oil; ^{1}H NMR (600 MHz, $CDCl_3$) δ 1.27 (t, J = 6.6 Hz, 3H), 1.39 (s, 9H), 2.90 (t, J = 7.2 Hz, 2H), 3.59 (t, J = 7.2 Hz, 2H), 4.18 (q, J = 6.6 Hz, 2H), 7.59 (d, J = 9.6 Hz, 1H), 7.98 (d, J = 6.6 Hz, 1H); ESI/MS, 447.4 (M + Na). Anal. Calcd for $C_{18}H_{20}FN_3O_4S_2$: C, 50.81; H, 4.74; N, 9.88. Found: C, 51.10; H, 4.64; N, 9.87.

Data for ***9h****:* yield, 63%; oil; ^{1}H NMR (600 MHz, $CDCl_3$) δ 1.25 (t, J = 7.2 Hz, 3H), 1.39 (s, 9H), 2.16−2.18 (m, 2H), 2.50 (t, J = 7.2 Hz, 2H), 3.41 (t, J = 7.2 Hz, 2H), 4.15 (q, J = 7.2 Hz, 2H), 7.59(*d*, J = 9.0 Hz, 1H), 7.98(*d*, J = 6.6 Hz, 1H). ESI/MS: 461.1(M+Na). Anal. Calcd for $C_{19}H_{22}FN_3O_4S_2$: C, 51.92; H, 5.05; N, 9.56. Found: C, 51.64; H, 5.01; N, 9.38.

Data for ***9i****:* yield, 49%; oil; ^{1}H NMR (600 MHz, $CDCl_3$) δ 1.20 (t, J = 6.6 Hz, 3H), 1.39 (s, 9H), 1.76 (s, 6H), 4.20 (q, J = 6.6 Hz, 2H), 7.61 (d, J = 9.0 Hz, 1H), 7.98 (d, J = 6.6 Hz, 1H); ESI/MS, 460.9 (M + Na). Anal. Calcd for $C_{19}H_{22}FN_3O_4S_2$: C, 51.92; H, 5.05; N, 9.56. Found: C, 51.62; H, 4.91; N, 9.47.

Data for ***9j****:* yield, 45%; oil; ^{1}H NMR (600 MHz, $CDCl_3$) δ 0.93 (t, J = 7.8 Hz, 3H), 1.39 (s, 9H), 1.68−1.69 (m, 2H), 4.14 (t, J = 6.6 Hz, 2H), 4.17 (s, 2H), 7.59 (d, J = 9.0 Hz, 1H), 7.98 (d, J = 6.6 Hz, 1H); ESI/MS, 447.3 (M + Na). Anal. Calcd for $C_{18}H_{20}FN_3O_4S_2$: C, 50.81; H, 4.74; N, 9.88. Found: C, 50.93; H, 4.96; N, 9.93.

Data for ***9k****:* yield, 62%; mp, 125−127 °C; ^{1}H NMR (600 MHz, $CDCl_3$) δ 1.39 (s, 9H), 4.08 (d, J = 7.8 Hz, 2H), 6.26 (t, J = 7.8 Hz, 1H), 7.60 (d, J = 9.0 Hz, 1H), 7.98 (d, J = 6.6 Hz, 1H); ESI/MS, 455.2 (M + Na). Anal. Calcd for $C_{16}H_{14}C_{l2}FN_3O_2S_2$: C, 44.24; H, 3.25; N, 9.67. Found: C, 44.47; H, 3.36; N, 9.84.

Data for ***9l****:* yield, 62%; mp, 82−84 °C; ^{1}H NMR (600 MHz, $CDCl_3$) δ 1.26 (t, J = 6.6 Hz, 3H), 1.39 (s, 9H), 1.71 (d, J = 7.2 Hz, 2H), 4.22 (q, J = 6.6 Hz, 2H), 4.67 (q, J = 7.2 Hz, 2H), 7.60 (d, J = 9.6 Hz, 1H), 7.98 (d, J = 6.6 Hz, 1H); ESI/MS, 447.0 (M + Na). Anal. Calcd for $C_{18}H_{20}FN_3O_4S_2$: C, 50.81; H, 4.74; N, 9.88. Found: C, 50.59; H, 4.55; N, 9.69.

Data for ***9m****:* yield, 64%; mp, 102−104 °C; ^{1}H NMR (600 MHz, $CDCl_3$) δ 1.39 (s, 9H), 3.73 (s, 3H), 4.11 (d, J = 7.2 Hz, 2H), 6.10 (d, J = 15.6 Hz, 2H), 7.04−7.07 (m, 1H), 7.60 (d, J = 9.0 Hz, 1H), 8.0 (d, J = 6.6 Hz, 1H); ESI/MS, 444.9 (M + Na). Anal. Calcd for $C_{18}H_{18}FN_3O_4S_2$: C, 51.05; H, 4.28; N, 9.92. Found: C, 51.26; H, 4.34; N, 10.03.

Data for ***9n****:* yield, 67%; mp, 97−99 °C; ^{1}H NMR (600 MHz, $CDCl_3$) δ 1.27 (d, J = 6.0 Hz, 6H), 1.39 (s, 9H), 4.12 (s, 2H), 5.08−5.10 (m, 1H), 7.60 (d, J = 7.4 Hz, 1H), 7.95 (d, J = 6.6 Hz, 1H); ESI/MS, 447.7 (M + Na). Anal. Calcd for $C_{18}H_{20}FN_3O_4S_2$: C, 50.81; H, 4.74; N, 9.88. Found: C, 51.07; H, 4.82; N, 9.95.

Data for ***10a****:* yield, 89%; mp 110−111 °C; ^{1}H NMR (600 MHz, $CDCl_3$) δ 1.28 (t, J = 6.6 Hz, 3H), 1.39 (s, 9H), 4.16 (s, 2H), 4.24 (q, J = 6.6 Hz, 2H), 7.95 (s, 1H), 8.07 (s, 1H); ESI/MS, 493.9 (M + Na). Anal. Calcd for $C_{17}H_{18}BrN_3O_4S_2$: C, 43.22; H, 3.84; N, 8.90. Found: C, 43.43; H, 4.04; N, 8.92.

Data for ***10b****:* yield, 88%; mp, 125−127 °C; ^{1}H NMR (600 MHz, $CDCl_3$) δ 1.39 (s, 9H), 3.79 (s, 3H), 4.18 (s, 2H), 7.96 (s, 1H), 8.07 (s,1H); ESI/MS, 479.7 (M + Na). Anal. Calcd for $C_{16}H_{16}BrN_3O_4S_2$: C, 41.93; H, 3.52; N, 9.17. Found: C, 42.05; H, 3.69; N, 9.33.

Data for ***10c****:* yield 75%; mp, 116−118 °C; ^{1}H NMR (600 MHz, $CDCl_3$) δ 1.26 (d, J = 6.0 Hz, 6H), 1.39 (s, 9H), 4.13 (s, 2H), 5.08 (m, 1H), 7.93 (s, 1H), 8.07 (s, 1H); ESI/MS, 507.7 (M + Na). Anal. Calcd for $C_{18}H_{20}BrN_3O_4S_2$: C, 44.45; H, 4.14; N, 8.64. Found: C, 44.19; H, 4.11; N, 8.44.

Data for ***10d****:* yield, 61%; oil; ^{1}H NMR (400 MHz, $CDCl_3$) δ 1.25 (t, J = 7.2 Hz, 3H), 1.39 (s, 9H), 2.17−2.19 (m, 2H), 2.49 (t, J = 7.2 Hz, 2H), 3.41 (t, J = 7.2 Hz, 2H), 4.13 (q, J = 7.2 Hz, 2H), 7.95 (s, 1H), 8.06 (s, 1H); ESI/MS, 500.4 (M + H). Anal. Calcd for $C_{19}H_{22}BrN_3O_4S_2$: C, 45.60; H, 4.43; N, 8.40. Found: C, 45.43; H, 4.33; N, 8.32.

Data for ***10e****:* yield, 35%; oil; ^{1}H NMR (400 MHz, $CDCl_3$) δ 1.25 (t, J = 7.2 Hz, 3H), 1.39 (s, 9H), 1.71 (d, J = 7.2 Hz, 3H), 4.22 (q, J = 7.2 Hz, 2H), 4.69 (q, J = 7.2 Hz, 1H), 7.95 (s, 1H), 8.07 (s,1H); ESI/MS, 486.2 (M^+). Anal. Calcd for $C_{18}H_{20}BrN_3O_4S_2$: C, 44.45; H, 4.14; N, 8.64. Found: C, 44.58; H, 4.19; N, 8.80.

Data for ***10f****:* yield, 79%; oil; ^{1}H NMR (400 MHz, $CDCl_3$) δ 1.26 (t, J = 7.2 Hz, 3H), 1.39 (s, 9H), 2.89 (t, J = 6.8 Hz, 2H), 3.59 (t, J = 6.8 Hz, 2H), 4.69 (q, J = 7.2 Hz, 2H), 7.96 (s, 1H), 8.06 (s, 1H); ESI/MS, 486.1 (M^+). Anal. Calcd for $C_{18}H_{20}BrN_3O_4S_2$: C, 44.45; H, 4.14; N, 8.64. Found: C, 44.69; H, 4.25; N, 8.85.

Data for ***10g****:* yield, 46%; oil; ^{1}H NMR (400 MHz, $CDCl_3$) δ 0.92 (t, J = 7.6 Hz, 3H), 1.39 (s, 9H), 1.67−1.69 (m, 2H), 4.13 (t, J = 6.8 Hz, 2H), 4.17 (s, 2H), 7.94 (s, 1H), 8.07 (s, 1H); ESI/MS, 487.3 (M + H). Anal. Calcd for $C_{18}H_{20}BrN_3O_4S_2$: C, 44.45; H, 4.14; N, 8.64. Found: C, 44.33; H, 3.95; N, 8.45.

Data for ***10h****:* yield, 73%; oil; ^{1}H NMR (400 MHz, $CDCl_3$) δ 1.39 (s, 9H), 2.30 (t, J = 2.8 Hz, 1H), 4.13 (d, J = 2.8 Hz, 2H), 8.00 (s, 1H), 8.09 (s,1H); ESI/MS, 424.3 (M^+). Anal. Calcd for $C_{16}H_{14}BrN_3O_2S_2$: C, 45.29; H, 3.33; N, 9.90. Found: C, 45.19; H, 3.24; N, 9.67.

Data for ***10i****:* yield, 53%; oil; ^{1}H NMR (400 MHz, $CDCl_3$) δ 1.40 (s, 9H), 4.10 (d, J = 7.2 Hz, 2H), 6.27 (s, 1H), 7.99 (s, 1H), 8.10 (s,1H); ESI/MS, 495.6 (M^+). Anal. Calcd for $C_{16}H_{14}BrCl_2N_3O_2S_2$: C, 38.80; H, 2.85; N, 8.48. Found: C, 39.08; H, 2.97; N, 8.69.

X-ray Diffraction. Colorless blocks of **8e** (0.23 mm × 0.12 mm × 0.10 mm) were counted on a quartz fiber with protection oil. Cell dimensions and intensities were measured at 300 K on a Bruker SMART CCD area detector diffractometer with graphite monochromated Mo Kα radiation (λ = 0.71073 Å); θ_{max} = 26.5°; 10109 measured reflections; 4538 independent reflections (R_{int} = 0.040) of which 3683 had $I > 2\sigma(I)$. Data were corrected for Lorentz and polarization effects and for absorption (T_{min} = 0.9160; T_{max} = 0.9622). The structure was solved by direct methods using SHELXS-97 (*28*); all other calculations were performed with Bruker SAINT System and Bruker SMART programs (*29*). Full-matrix least-squares refinement based on F^2 using the weight of $1/[\sigma^2(F_o^2) + (0.0786P)^2 + 0.3001P]$ gave final values of R = 0.049, ωR = 0.153, and GOF(F) = 1.106 for 386 variables and 2650 contributing reflections. Maximum shift/error = 0.000(3), and max/min residual electron density = 1.201/−1.297 e Å^{-3}. Hydrogen atoms were observed and refined with a fixed value of their isotropic displacement parameter.

Enzyme Expression, Purification, and Inhibition Kinetic Analysis. Recombinant human PPO was expressed by using the pTrcHis vector and purified according to reported methods (*3*, *30*, *31*). The pTrcHis (PPO) plasmid was transformed into *Escherichia coli* JM109. Transformed cells carrying pTrcHis (PPO) were inoculated into 0.5 L of 2× YT grown at 37 °C with 200 rpm shaking until an A_{600} of 0.6 was reached. The expression of the recombinant PPO enzyme was induced by adding isopropyl β-D-1-thiogalactopyranoside (IPTG, 1 mM). Cells were grown for an additional 4 h at 25 °C, harvested by centrifugation, resuspended in 50 mM Tris buffer (pH 8.0) containing 0.5 M NaCl, 1 μg/mL phenylmethanesulfonyl fluoride (PMSF), and 0.2% (v/v) Triton X-100, and then disrupted by sonication. Cellular debris was removed by centrifugation at 12500 rpm. The supernatant was subjected to Ni-affinity chromatography. Protein concentrations were determined according to the method of Bradford with bovine serum albumin (BSA) as a standard (*32*). PPO activity was assayed by fluorescence as described previously (*33*−*36*). The product has a maximum excitation wavelength at 410 nm and a maximum emission wavelength at 630 nm. The total volume of the reaction mixture was 200 μL consisting of 0.1 M potassium phosphate buffer (pH 7.4), 5 mM dithiothreitol (DTT), 1 mM EDTA, 0.2 M imidazole, and 0.03% Tween 80 (v/v). The enzymatic reaction was started by the addition of substrate. The autoxidation rates were determined concomitantly and were subsequently subtracted. The concentration of protoporphyrinogen IX was determined by the difference of the absorption of protoporphyrin IX before and after the complete enzyme oxidation of the substrate monitored by UV−vis spectrophotometer at a wavelength of 410 nm. The concentration of protoporphyrin IX was calculated from the calibration graph. In assays, the inhibitors were added from a stock solution in dimethyl sulfoxide (DMSO) and then added 1% total volume in each assay. The final concentration ranged from 0.005 to 250 μM.

The kinetic parameters were evaluated by Sigma Plot software 10.0 (SPSS, Chicago, IL). IC_{50} was determined by measuring PPO activity over a range of inhibitor concentrations at a single substrate concentration. IC_{50} values were calculated by fitting v versus [I] data to a single binding site model described by eq 1

$$y = \min + \frac{\max - \min}{1 + 10^{\log IC_{50} - x}} \quad (1)$$

where y is the percentage of maximal rate, max and min are the y values at which the curve levels off, x is the logarithm of inhibitor concentration, and IC_{50} is the inhibitor concentration that elicits 50% of the total inhibition. The calculated K_i value is obtained by applying the following

relationship, which exists for competitive inhibition among K_i, K_m, and IC_{50} at any saturating substrate concentration (S).

$$K_i = \frac{IC_{50}}{S/K_m + 1} \quad (2)$$

CoMSIA Analysis. Comparative molecular similarity indices analysis (CoMSIA) (*37*) was applied to understand the QSAR of the compounds tested in this study. The 3D structures of all compounds were built on the basis of the crystal structure of **8e** and then minimized by using SYBYL 7.1 on a Silicon Graphics Fuel workstation. The geometries of all molecules involved in this study were fully optimized by using the PM3 method. The lowest energy conformations were considered as the bioactive conformations. A useful kind of net atomic charges called electrostatic potential (ESP) fitting charges were derived from the PM3 calculated molecular electrostatic potential distribution. The common framework of benzothiazole and 1,3,4-oxadiazole-2(3*H*)-one ring was selected as the template to superimpose all of the compounds using an atom-by-atom least-squares fit implemented in the SYBYL FIT option in SYBYL. **8c** with the best biological activity was selected as the reference molecule. CoMSIA similarity index descriptors $A_{F,k}$ for a molecule j with atoms i at the grid point q are determined as

$$A^q_{F,k}(j) = \sum_i \omega_{probe,k}\omega_{ik}\, e^{-\alpha r^2_{iq}} \quad (3)$$

where ω_{ik} is the actual value of the physicochemical property k (steric, electrostatic, hydrophobic), which was evaluated using the probe atom. A Gaussian type distance dependence was used between the grid point q and each atom i of the molecule. The default value of 0.3 was used as the attenuation factor α. An sp^3 carbon atom with +1.0 charge served as the probe atom to calculate steric, electrostatic, and hydrophobic fields. Two angstrom grid point spacing was used. The all-orientation search (AOS) method was used for CoMSIA analysis. The AOS routine (*38*) optimizes the field sampling by rotating the molecular aggregate systematically and picking the orientation that produces the highest q^2 value. Details of the AOS routine were described previously (*37*, *39*). Briefly, the whole aggregate was rotated about the x, y, and z axes systematically with an increment of 30° using the STATIC ROTATE command. For each orientation, a conventional CoMSIA was performed as described above and the predictive value of the model was evaluated using leave-one-out (LOO) cross-validation with sample-distance partial least-squares (SAMPLS). The orientation that gave the highest q^2 value was selected to produce the final model. A Sybyl Programming language (SPL) script was written to perform the AOS routine as described (*39*) automatically.

Greenhouse Herbicidal Activities. The herbicidal activities of series **8**, **9**, and **10** against monocotyledon weeds such as *Echinochloa crus-galli* (EC), *Digitaria sanguinalis* (DS), and *Poa annua* (PA) and dicotyledon weeds such as *Brassica juncea* (BJ), *Amaranthus retroflexus* (AR), and *Eclipta prostrate* (EP) were evaluated according to a previously reported procedure (*40*−*42*). Sulfentrazone was selected as a positive control because it is one of the few soil-active PPO inhibitors (*43*−*45*). All test compounds were formulated as 100 g/L emulsified concentrates by using DMF as solvent and Tween-80 as emulsification reagent. The concentrated formulas were diluted with water to the required concentration and applied to pot-grown plants in a greenhouse. The soil used was a clay soil, pH 6.5, 1.6% organic matter, 37.3% clay particles, and CEC = 12.1 mol/kg. The rate of application (g. of ai/ha) was calculated by the total amount of active ingredient in the formulation divided by the surface area of the pot. Plastic pots with a diameter of 9.5 cm were filled with soil to a depth of 8 cm. Approximately 20 seeds of the tested weeds were sown in the soil at the depth of 1−3 cm and grown at 15−30 °C in a greenhouse. The air relative humidity is 50%. The diluted formulation solutions were applied for postemergence treatment; dicotyledon weeds were treated at the two-leaf stage, and monocotyledon weeds were treated at the one-leaf stage, respectively. The postemergence application rate was 150 g of ai/ha. Untreated seedlings were used as the control group, and solvent (DMF + Tween-80) treated seedlings were used as the solvent control group. Herbicidal activity was evaluated visually 15 days after treatment. The results of herbicidal activities are shown in **Table 1**, three replicates per treatment. Seven kinds of dicotyldon weeds, such as *B. juncea*, *Polygonum humifusum*, *Abutilon theophrasti*, *Cyperus iria*, *A. retroflexus*, *Rumex acetasa*, and *E. prostrate* were used for the further test of **8c**, **8h**, **9d**, **9h**, **9j**, **9l**, **9n**, and **10b**.

Table 1. PPO Inhibition and Herbicidal Activity of Series **8**, **9**, and **10**

				postemergence,[a] 150 g of ai/ha					
no.	X	R	k_i (μM)	EC	DS	PA	BJ	AR	EP
8a	Cl	CH_2CHCCl_2	10.24	0	0	0	70	70	40
8b	Cl	$COOCH_2CH_3$	0.33	0	0	0	70	70	40
8c	Cl	$CH_2CH_2COOCH_2CH_3$	0.25	0	0	0	70	**80**	60
8d	Cl	$CH_2COOCH_2CH_3$	1.01	0	0	0	50	70	60
8e	Cl	$CH_2COOC(CH_3)_3$	0.84	0	0	0	50	40	30
8f	Cl	CH_2COOCH_3	1.07	0	0	0	0	70	50
8g	Cl	$CH_2CH_2CH_2COOCH_2CH_3$	2.02	0	0	0	0	50	0
8h	Cl	$CH(CH_3)COOCH_2CH_3$	1.69	0	0	0	50	**100**	70
8i	Cl	$CH_2CH{=}CH_2$	3.11	0	0	0	70	70	60
8j	Cl	$C(CH_3)_2COOCH_2CH_3$	1.35	0	0	0	60	50	50
8k	Cl	$CH_2COOCH(CH_3)_2$	2.17	0	0	0	0	50	0
8l	Cl	$CH_2COOCH_2CH_2CH_3$	0.98	0	0	0	0	70	0
8m	Cl	CH_2CCH	8.61	/[b]	/	/	/	/	/
9a	F	CH_2COOCH_3	3.99	0	0	0	0	60	0
9b	F	$COOCH_3$	0.72	0	0	0	0	40	0
9c	F	$COOCH_2CH_3$	1.30	0	0	0	0	0	0
9d	F	$CH_2COOCH_2CH_3$	1.58	0	0	0	50	**90**	50
9e	F	$CH_2COOC(CH_3)_3$	1.59	0	0	0	0	0	0
9f	F	$CH_2CH{=}CH_2$	15.92	0	0	0	60	60	40
9g	F	$CH_2CH_2COOCH_2CH_3$	0.32	0	0	0	60	50	50
9h	F	$CH_2CH_2CH_2COOCH_2CH_3$	0.70	0	0	0	50	**90**	70
9i	F	$C(CH_3)_2COOCH_2CH_3$	1.54	0	0	0	50	60	70
9j	F	$CH_2COOCH_2CH_2CH_3$	0.70	0	0	0	50	**100**	**90**
9k	F	CH_2CHCCl_2	10.92	50	40	50	70	60	60
9l	F	$CH(CH_3)COOCH_2CH_3$	1.42	0	50	50	75	**90**	**95**
9m	F	$CH_2CH{=}CHCOOCH_3$	7.48	0	0	0	40	40	50
9n	F	$CH_2COOCH(CH_3)_2$	1.17	0	0	0	40	**90**	70
10a	Br	$CH_2COOCH_2CH_3$	6.96	0	0	0	0	75	0
10b	Br	CH_2COOCH_3	7.46	0	0	0	0	**80**	0
10c	Br	$CH_2COOCH(CH_3)_2$	5.97	0	0	0	0	75	0
10d	Br	$CH_2CH_2CH_2COOCH_2CH_3$	5.83	/	/	/	/	/	/
10e	Br	$CH(CH_3)COOCH_2CH_3$	8.13	0	0	0	0	70	60
10f	Br	$CH_2CH_2COOCH_2CH_3$	1.69	0	0	0	0	0	30
10g	Br	$CH_2COOCH_2CH_2CH_3$	3.10	0	0	0	0	50	30
10h	Br	CH_2CCH	11.12	0	0	0	40	40	40
10i	Br	CH_2CHCCl_2	18.63	/	/	/	/	/	/
sulfentrazone			0.72	75	70	/	**100**	**100**	**100**

[a] EC, *Echinochloa crus-galli*; DS, *Digitaria sanguinalis*; PA, *Poa annua*; BJ, *Brassica juncea*; AR, *Amaranthus retroflexus*; EP, *Eclipta prostrata*. [b] /, not tested.

RESULTS AND DISCUSSION

Synthesis of the Title Compounds. As shown in **Scheme 2**, the target series **8**, **9**, and **10** were prepared by a seven-step synthetic route. The preparation of intermediates **2**, **3**, **4**, and **5** was easily obtained according to existing methods and resulted in good to excellent yields. After obtaining intermediates **5**, we tried to prepare intermediate **7** directly from series **5** according to the reported method (*46*). However, the reaction of intermediate **5** with sodium polysulfide and carbon disulfide was so complex that it is difficult to isolate the desired product in good yield. However, the use of iron powder to reduce intermediate **5** into **6**, which underwent ring-closing reaction with potassium *O*-ethyl carbonodithioate in the DMF solution, produced the key intermediate **7** in acceptable yields (53−60%). Finally, intermediates **7a**−**c** reacted with various alkylation reagents to give the target series **8**, **9**, and **10** in yields of 35−89%. The structures of all intermediates and title compounds were confirmed by elemental analyses, ^1H NMR, and ESI-MS spectral data. In addition, the crystal structure of **8e** was determined by X-ray diffraction analyses. As shown in **Figure 2**, the dihedral angle between the benzothiazole ring (max deviation = 0.013 Å) and 1,3,4-oxadiazol-2(3*H*)-one ring is 58.69°. The crystal packing is stabilized by two intermolecular hydrogen-bonding (C−H···O) interactions.

In Vitro Activity and CoMSIA Analysis. The k_i values against human PPO of the synthesized compounds **8**−**10** are listed in **Table 1**. Sulfentrazone, a commercial PPO inhibitor, was used as a positive control. For the sake of clarity, **8a**−**m**, **9a**−**n**, and **10a**−**i** will be named as chlorine, fluorine, and bromine derivatives, respectively, throughout the text. Results as shown in **Table 1** indicated that **8c** (k_i = 0.25 μM) displayed the highest PPO inhibitory activity, about 3 times higher than that of sulfentrazone (k_i = 0.72 μM). Generally speaking, series **10** (X = Br) always displayed a much lower PPO inhibitory activity than series **8** (X = Cl) and **9** (X = F) containing the same R group, for example, **8a**, **9k**, and **10i** (R = CH_2CHCCl_2), **8c**, **9g**, and **10f** (R = $CH_2CH_2COOCH_2CH_3$), **8d**, **9d**, and **10a** (R = $CH_2COOCH_2CH_3$). However, series **8** sometimes displayed higher activity than series **9** containing the same R group but sometimes lower activity than the corresponding analogues **9**. For example, **8b**, **8c**, 8d, **8e**, **8f**, **8i**, and **8j** displayed higher activity than the corresponding **9c**, **9g**, **9d**, **9e**, **9a**, **9f**, and **9i**. In addition, **Table 1** also shows that $CH_2CH_2COOCH_2CH_3$ is the best group for the R position among the investigated substituents, because **8c**, **9g**, and **10f** displayed the highest activity within the chlorine, fluorine, and bromine derivatives, respectively.

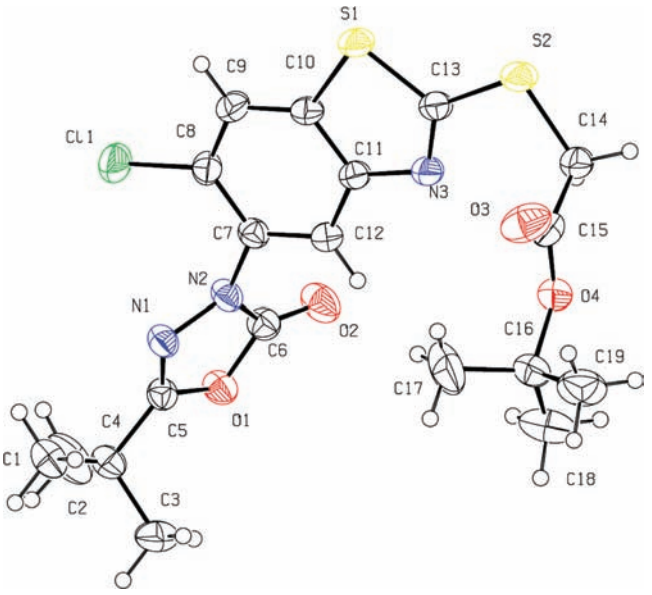

Figure 2. Crystal structure of **8e**.

To understand the substituent effects on the PPO inhibition of these compounds, the method of CoMSIA was applied to understand the quantitative structure−activity relationships. As listed in **Table 2**, a predictive CoMSIA model was established with the conventional correlation coefficient r^2 = 0.933 and the cross-validated coefficient q^2 = 0.585; the contributions of steric, electrostatic, and hydrophobic fields are 19.0, 47.5, and 33.5%, respectively. The observed and calculated activity values for all of the compounds are given in **Table 3**, and the plots of the predicted versus the actual activity values for all of the compounds are shown in **Figure 3**. In **Figures 4**, **5**, and **6**, the isocontour diagrams of the steric, electrostatic, and hydrophobic field contributions ("stdev*coeff") obtained from the CoMSIA analysis are illustrated together with exemplary ligands. The steric field contour map is plotted in **Figure 4**. The green region highlights positions where a bulky group would be favorable for higher PPO inhibition activity. In contrast, yellow indicates positions where a decrease in the bulk of the desired compounds is favored. As shown in **Figure 4**, the CoMSIA steric contour plots indicated that a yellow region is located around the side chain of the benzothiazolyl group, whereas a green region is near the carboxyl oxygen atom. This map means that the substituents at this position should have an optimum steric effect, which supports **8c** (R = $CH_2CH_2COOC_2H_5$, k_i = 0.25 μM) being more active than **8d** (R = $CH_2COOC_2H_5$, k_i = 1.01 μM) and **8g** (R = $CH_2CH_2CH_2COOC_2H_5$, k_i = 2.02 μM). The electrostatic contour plot is shown in **Figure 5**. The blue contour defines a region where an increase in the positive charge will result in an increase in the activity, whereas the red contour defines a region of space where increasing electron density is favorable. As shown in **Figure 5**, the target compounds bearing an electron-withdrawing

Scheme 2. Synthetic Route for the Title Compounds **8**, **9**, and **10**

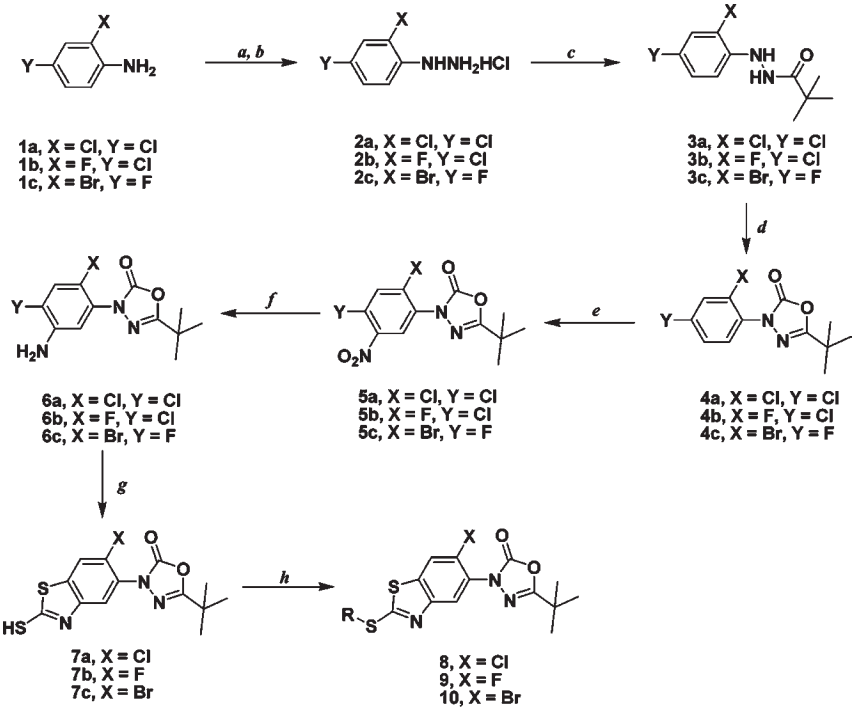

Table 2. Summary of CoMSIA Analysis

					contribution (%)		
q_{cv}^2	$r_{n\text{-}cv}^2$	s	F	comp	steric	electrostatic	hydrophobic
0.585	0.933	0.142	67.706	6	19.0	47.5	33.5

Table 3. Results of the Experimental and Calculated k_i Values

	pk_i[a]			pk_i[a]	
no.	expt	calcd	no.	exptl	calcd
8a	4.99	5.15	**9f**	4.80	5.12
8b	6.48	6.29	**9g**	6.49	6.42
8c	6.60	6.55	**9h**	6.15	6.15
8d	6.00	6.04	**9i**	5.81	5.83
8e	6.08	6.16	**9j**	6.15	6.03
8f	5.97	6.03	**9k**	4.96	4.86
8g	5.69	5.62	**9l**	5.85	5.63
8h	5.77	5.75	**9m**	5.13	5.02
8i	5.51	5.28	**9n**	5.93	5.87
8j	5.87	5.87	**10a**	5.16	5.24
8k	5.66	5.78	**10b**	5.13	5.10
8l	6.01	5.99	**10c**	5.22	5.25
8m	5.06	5.17	**10d**	5.23	5.19
9a	5.40	5.27	**10e**	5.09	5.34
9b	6.14	6.17	**10f**	5.77	5.67
9c	5.89	6.20	**10g**	5.51	5.63
9d	5.80	5.76	**10h**	4.95	4.92
9e	5.80	5.79	**10i**	4.73	4.63

[a] pk_i = −log k_i.

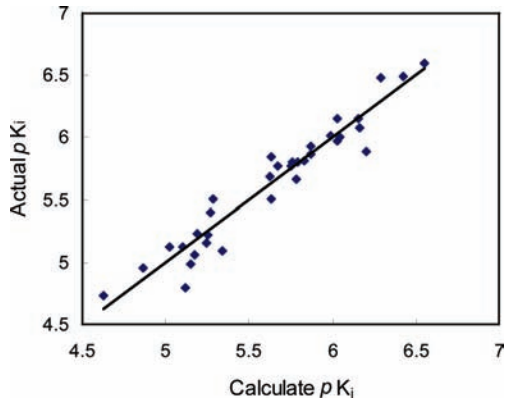

Figure 3. CoMSIA predicted as experimental pK_i values.

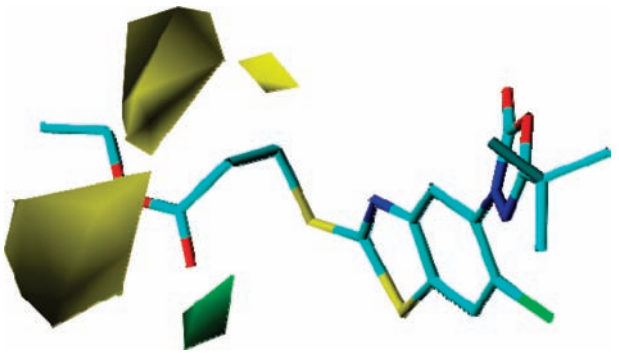

Figure 4. Steric map from the CoMSIA model. **8c** is shown inside the field. Sterically favored areas (0.030 level) are represented by green polyhedra. Sterically disfavored areas (−0.004 level) are represented by yellow polyhedra.

group at the side chain of benzothiazole ring will display higher activity. For example, compounds containing an ester group

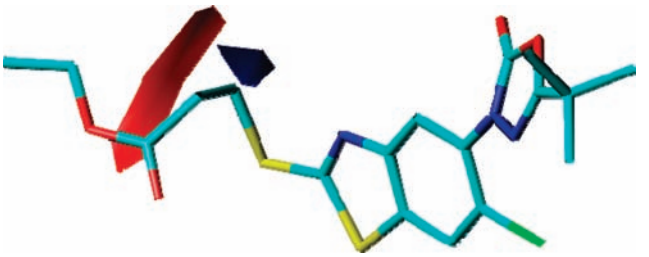

Figure 5. Electrostatic map from the CoMSIA model. **8c** is shown inside the field. Blue contours (0.070 level) encompass regions where an increase of positive charge will enhance affinity, whereas in red contoured areas (−0.040 level) more negative charges are favorable for binding properties.

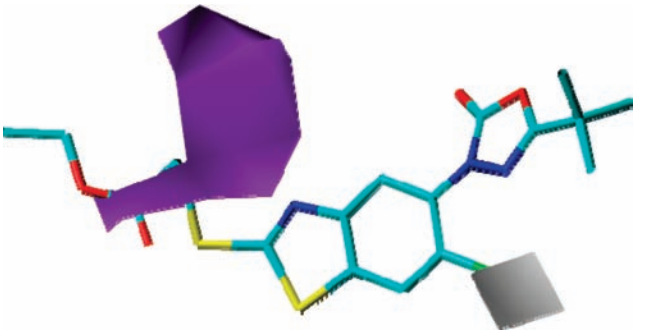

Figure 6. Hydrophobic map from the CoMSIA model. **8c** is shown inside the field. Violet contours (0.010 level) encompass regions where an increase of hydrophobic effect will enhance affinity, whereas in gray contoured areas (−0.050 level) a more hydrophilic effect is favorable for binding properties.

always displayed higher activity than the derivatives (**8a**, **8i**, **8m**, **9f**, **9k**, **10h**, and **10i**) bearing an alkyl group as side chain. As shown in **Figure 6**, violet regions indicate areas where hydrophobic groups increase activity, and gray regions indicate areas where hydrophilic groups will increase activity. Fluorine and chlorine atoms are more hydrophilic than bromine atoms; therefore, series **8** and **9** are always more active than series **10**. In addition, the ester group is hydrophobic, which accounts for why compounds containing an ester group always displayed higher activity. In fact, the PPO inhibition of chlorine derivatives **8a**−**m** displayed linear correlation with the hydrophobic effects to some extent (data not shown).

Greenhouse Herbicidal Activities. The postemergence herbicidal activity of series **8**, **9**, and **10** was tested in the greenhouse at a concentration of 150 g. of ai/ha; a triazolinone-type commercial product, sulfentrazone, was selected as a positive control. As shown in **Table 1**, no compound had herbicidal activity at the concentration of 150 g of ai/ha against *E. crus-galli*, *D. sanguinalis*, or *P. annus*. On the other hand, some of the series had good herbicidal activities against *B. juncea*, *A. retroflexus*, and *E. prostrate*. The inhibition effects of **8c**, **8h**, **9d**, **9h**, **9j**, **9l**, **9n**, and **10b** against *A. retroflexus* are >80%. Therefore, these eight compounds were selected for further test. As shown in **Table 4**, **9l** was the most promising candidate. Even at the concentration of 37.5 g of ai/ha, **9l** showed excellent herbicidal activity with broad spectrum. Its inhibition effects against *A. theophrasti*, *C. iria*, *R. acetasa*, and *E. prostrate* are >80%. At the same time, **9l** also displayed moderate herbicidal activity against *B. juncea*, *P. humifusum*, and *A. retroflexus* at the concentration of 37.5 g of ai/ha.

Table 4. Herbicidal Spectrum Test of Eight Selected Compounds (Postemergence)[a]

compd	dosage (g of ai/ha)	BJ	PH	AT	CI	AR	RA	EP
8c	37.5	60	70	0	40	50	60	50
	75	60	70	0	50	60	70	60
	150	60	70	0	60	80	70	60
8h	37.5	0	40	0	60	60	0	0
	75	0	60	0	60	100	30	40
	150	0	70	0	70	100	60	70
9d	37.5	0	70	0	60	50	50	0
	75	50	70	0	70	50	50	0
	150	50	80	0	70	90	70	50
9h	37.5	50	50	0	60	60	50	50
	75	50	80	0	60	80	60	60
	150	50	80	50	70	90	70	70
9j	37.5	50	60	0	40	0	50	0
	75	50	70	0	40	60	60	40
	150	50	80	0	60	100	70	90
9l	37.5	70	60	80	90	60	95	80
	75	70	70	100	90	60	95	85
	150	75	70	100	100	90	100	95
9n	37.5	40	40	0	50	0	50	0
	75	50	40	0	50	85	60	0
	150	50	60	0	60	90	70	70
10b	37.5	0	60	0	40	50	40	0
	75	0	70	0	40	60	50	0
	150	0	70	0	50	80	60	0

[a] BJ, *Brassica juncea*; PH, *Polygonum humifusum*; AT, *Abutilon theophrasti*; CI, *Cyperus iria*; AR, *Amaranthus retroflexus*; RA, *Rumex acetasa*; EP, *Eclipta prostrate*.

In summary, a series of 1,3,4-oxadiazol-2(3*H*)-ones containing benzothiazole substructure were designed and synthesized as potential PPO inhibitors. The results of in vitro and greenhouse tests indicated that series **8**, **9**, and **10** had good PPO inhibition activity and herbicidal activity at the concentration of 150 g of ai/ha. Most interestingly, **9l**, ethyl 2-((5-(5-*tert*-butyl-2-oxo-1,3,4-oxadiazol-2(3*H*)-yl)-6-fluorobenzothiazol-2-yl)sulfanyl)propanoate, was identified as the most promising candidate due to its high PPO inhibition effect (k_i = 1.42 μM) and broad-spectrum herbicidal activity at the concentration of 37.5 g of ai/ha. The crop selectivity and field trial of **9l** are under way.

ACKNOWLEDGMENT

We thank Dr. Jie Chen for the greenhouse test of biological activities.

LITERATURE CITED

(1) Duke, S. O.; Nandihalli, U. B.; Lee, H. J.; Duke, M. V. Protoporphyrinogen oxidase as the optimal herbicide site in the porphyrin pathway. *Am. Chem. Soc. Symp. Ser.* **1994**, *No. 559*, 191–204.

(2) Scalla, R.; Matringe, M. Inhibitors of protoporphyrinogen oxidase as herbicides: diphenyl ethers and related. *Rev. Weed Sci.* **1994**, *6*, 103–132.

(3) Manelia, M. H.; Corrigalla, A. V.; Klumpb, H. H.; Davidsa, L. M.; Kirscha, R. E.; Meissnera, P. N. Kinetic and physical characterisation of recombinant wild-type and mutant human protoporphyrinogen oxidases. *Biochim. Biophys. Acta* **2003**, *1650*, 10–21.

(4) Meazza, G.; Bettarini, F.; La Porta, P.; Piccardi, P.; Signorini, E; Portoso, D.; Fornara, L. Synthesis and herbicidal activity of novel heterocyclic protoporphyrinogen oxidase inhibitors. *Pest. Manag. Sci.* **2004**, *60*, 1178–1188.

(5) Dayan, F. E.; Green, H. M.; Weete, J. D.; Hancock, H. G. Postemergence activity of sulfentrazone: effects of surfactants and leaf surfaces. *Weed Sci.* **1996**, *44*, 797–803.

(6) Dayan, F. E.; Duke, S. O.; Weete, J. D.; Hancock, H. G. Selectivity and mode of action of carfentrazone-ethyl, a novel phenyl triazolinone herbicide. *Pestic. Sci.* **1997**, *51*, 65–73.

(7) Shapiro, R.; DiCosimo, R.; Hennessey, S. M.; Stieglitz, B.; Campopiano, O.; Chiang, G. C. Discovery and development of a commercial synthesis of azafenidin. *Org. Process Res. Dev.* **2001**, *5*, 593–598.

(8) Dayan, F. E.; Duke, S. O.; Reddy, K. N.; Hamper, B. C.; Leschinsky, K. L. Effects of isoxazole herbicides on protoporphyrinogen oxidase and porphyrin physiology. *J. Agric. Food Chem.* **1997**, *45*, 967–975.

(9) Hess, F. D. Light-dependent herbicides: an overview. *Weed Sci.* **2000**, *48*, 160–170.

(10) Dayan, F. E.; Duke, S. O. Phytotoxicity of protoporphyrinogen oxidase inhibitors: phenomenology, mode of action and mechanisms of resistance. In *Herbicide Activity: Toxicology, Biochemistry and Molecular Biology*; Roe, R. M., Burton, J. D., Kuhr, R. J., Eds.; IOS Press: Washington, DC, 1997; pp 11−35.

(11) Lehnen, L. P.; Sherman, T. D.; Becerril, J. M.; Duke, S. O. Tissue and cellular localization of acifluorfen-induced porphyrins in cucumber cotyledons. *Pestic. Biochem. Physiol.* **1990**, *37*, 239–248.

(12) Duke, S. O.; Kenyon, W. H. Peroxidizing activity determined by cellular leakage. In *Target Assays for Modern Herbicides and Related Compounds*; Böger, P., Sandmann, G., Eds.; Lewis Publishers: Boca Raton, FL, 1993; pp 61−66.

(13) Dayan, F. E.; Duke, S. O. Herbicides: Protoporphyrinogen oxidase inhibitors. In *Encyclopedia of Agrochemicals*; Plimmer, J. R., Gammon, D. W., Ragsdale, N. N., Eds.; Wiley: New York, 2003; Vol. 2, pp 850−863.

(14) Hwang, I. T.; Hong, K. S.; Choi, J. S.; Kim, H. R.; Jeon, D. J.; Cho, K. Y. Protoporphyrinogen IX-oxidizing activities involved in the mode of action of a new compound *N*-[4-chloro-2-fluoro-5-{3-(2-fluorophenyl)-5-methyl-4,5-dihydroisoxazol-5-yl-methoxyl}-phenyl]-3,4,5,6-tetrahydrophthalimide. *Pestic. Biochem. Physiol.* **2004**, *80*, 123–130.

(15) Dayan, F. E.; Meazza, G.; Bettarini, F.; Signorini, E.; Piccardi, P.; Romagni, J. G.; Duke, S. O. Synthesis, herbicidal activity, and mode of action of IR 5790. *J. Agric. Food Chem.* **2001**, *49*, 2302–2307.

(16) Gitsopoulos, T. K.; Froud-Williams, R. J. Effects of oxadiargyl on direct-seeded rice and *Echinochloa crus-galli* under aerobic and anaerobic conditions. *Weed Res.* **2004**, *44*, 329–334.

(17) Hutchinson, I.; Jennings, S. A.; Vishnuvajjala, B. R.; Westwell, A. D.; Stevens, M. F. G. Antitumor benzothiazoles. 16. Synthesis and pharmaceutical properties of antitumor 2-(4-aminophenyl)-benzothiazole amino acid prodrugs. *J. Med. Chem.* **2002**, *45*, 744.

(18) Mortimer, C. G.; Wells, G.; Crochard, J.; Stone, E. L.; Bradshaw, T. D.; Stevens, M. F. G.; Westwell, A. D. Antitumor benzothiazoles. 26. 2-(3,4-Dimethoxyphenyl)-5-fluoro-benzothiazole (GW 610, NSC 721648), a simple fluorinated 2-arylbenzothiazole, shows potent and selective inhibitory activity against lung, colon, and breast cancer cell lines. *J. Med. Chem.* **2006**, *49*, 179.

(19) Huang, W.; Zhao, P. L.; Liu, C. L.; Chen, Q.; Liu, Z. M.; Yang, G. F. Design, synthesis and fungicidal activities of new strobilurin derivatives. *J. Agric. Food Chem.* **2007**, *55*, 3004–3010.

(20) Huang, W.; Tan, Y.; Ding, M. W.; Yang, G. F. An improved synthesis of 2-(3H)benzo- thiazolethiones under microwave irradiation. *Synth. Commun.* **2007**, *37*, 369–376.

(21) Huang, W.; Yang, G. F. Microwave-sssisted, one-pot syntheses and fungicidal activity of polyfluorinated 2-benzylthiobenzothiazoles. *Bioorg. Med. Chem.* **2006**, *14*, 8280–8285.

(22) Dekeyser, M. A.; Canada, W.; McDonald, P. T.; Conn, M. Insecticidal phenylhydrazine derivatives. U.S. Patent 5367093, 1994; *Chem. Abstr.* **1994**, *123*, 9144.

(23) Bullock, M. W.; Hand, J. J. Synthesis of some substituted indole-3-butyric acids. *J. Am. Chem. Soc.* **1956**, *78*, 5854–5857.

(24) Sawada, Y.; Yanai, T.; Nakagawa, H.; Tsukamoto, Y.; Yokoi, S.; Yanagi, M.; Toya, T.; Sugizaki, H.; Kato, Y.; Shirakura, H.;

Watanabe, T.; Yajima, Y.; Kodama, S.; Masui, A. Synthesis and insecticidal activity of benzoheterocyclic analogues of *N*′-benzoyl-*N*-(*tert*-butyl)benzohydrazide: part 2. Introduction of substituents on the benzene rings of the benzoheterocycle moiety. *Pest Manag. Sci*. **2003**, *59*, 36–48.

(25) Fischer, R.; Jensen-Korte, U.; Kunisch, F.; Marhold, A.; Ooms, P.; Schallner, O.; Santel, H. J.; Schmidt, R. R.; Krauskopf, B.; Strang, R. H. *N*-Aryl-substituted nitrogencontaining heterocycles, processes and novel intermediates for their preparation, and their use as herbicides and plant growth regulators. U.S. Patent 6906006, 2005; *Chem. Abstr*. **2005**, *143*, 21460.

(26) Bosch, J.; Roca, T.; Catena, J. L.; Farrerons, C.; Miquel, I. A convergent route to 5-(arylsulfanyl)-6-sulfonamido-3-benzofuranones. *Synthesis* **2000**, 721–725.

(27) Zhu, L.; Zhang, M. B.; Dai, M. A convenient synthesis of 2-mercapto and 2-chlorobenzo-thiazoles. *J. Heterocycl. Chem*. **2005**, *42*, 727.

(28) Sheldrick, G. M. *SHELXTL* (*Version 5.0*); University of Göttingen: Göttingen, Sweden, 2001.

(29) *SMART V5.628, SAINT V6.45, and SADABS*; Bruker AXS: Madison, WI, 2001.

(30) Dailey, T. A.; Dailey, T. A. Human protoporphyrinogen oxidase: expression, purification, and characterization of the cloned enzyme. *Protein Sci*. **1996**, *5*, 98–105.

(31) Corrigall, A. V.; Siziba, K. B.; Maneli, M. H.; Shephard, E. G.; Ziman, M.; Dailey, T. A.; Dailey, H. A.; Kirsch, R. E.; Meissner, P. N. Purification of and kinetic studies on a cloned protoporphyrinogen oxidase from the aerobic bacterium *Bacillus subtilis*. *Arch. Biochem. Biophys*. **1998**, *358*, 251–256.

(32) Berezovski, M.; Krylov, S. N. Using nonequilibrium capillary electrophoresis of equilibrium mixtures for the determination of temperature in capillary electrophoresis. *Anal. Chem*. **2004**, *76*, 7114–7117.

(33) Meissner, P. N.; Day, R. S.; Moore, M. R.; Disler, P. B.; Harley, E. Protoporphyrinogen oxidase and porphobilinogen deaminase in variegate porphyria. *Eur. J. Clin. Invest*. **1986**, *16*, 257–261.

(34) Shepherd, M.; Dailey, H. A. A continuous fluorimetric assay for protoporphyrinogen oxidase by monitoring porphyrin accumulation. *Anal. Biochem*. **2005**, *344*, 115–121.

(35) Jeong, E.; Houn, T. A point mutation of valine-311 to methionine in *Bacillus subtilis* protoporphyrinogen oxidase does not greatly increase resistance to the diphenyl ether herbicide oxyfluorfen. *Bioorg. Chem*. **2003**, *31*, 389–397.

(36) Tan, Y.; Sun, L.; Xi, Z.; Yang, G. F.; Jiang, D. Q.; Yan, X. P.; Yang, X.; Li, H. Y. A capillary electrophoresis assay for protoporphyrinogen oxidase. *Anal. Biochem*. **2008**, *383*, 200–204.

(37) Klebe, G.; Abraham, U.; Mietzner, T. Molecular similarity indices in a comparative analysis (CoMSIA) of drug molecules to correlate and predict their biological activity. *J. Med. Chem*. **1994**, *37*, 4130–4146.

(38) Wang, R.; Gao, Y.; Liu, L.; Lai, L. All-orientation search and all-placement search in comparative molecular field analysis. *J. Mol. Model*. **1998**, *4*, 276–283.

(39) Gangjee, A.; Lin, X. CoMFA and CoMSIA analyses of *Pneumocystis carinii* dihydrofolate reductase, *Toxoplasma gondii* dihydrofolate deductase, and rat liver dihydrofolate reductase. *J. Med. Chem*. **2005**, *48*, 1448–1469.

(40) Chen, C. N.; Lv, L. L.; Ji, F. Q.; Chen, Q.; Xu, H.; Niu, C. W.; Xi, Z.; Yang, G. F. Design and synthesis of *N*-2,6-difluorophenyl-5-methoxyl-1,2,4-triazolo[1,5-a]pyrimidine-2- sulfonamide as acetohydroxyacid synthase inhibitor. *Bioorg. Med. Chem*. **2009**, *17*, 3011–3017.

(41) Luo, Y. P.; Jiang, L. L.; Wang, G. D.; Chen, Q.; Yang, G. F. Syntheses and herbicidal activities of novel triazolinone derivatives. *J. Agric. Food Chem*. **2008**, *56*, 2118–2124.

(42) Li, Y. X.; Luo, Y. P.; Xi, Z.; Niu, C. W.; He, Y. Z.; Yang, G. F. Design and syntheses of novel phthalazin-1(2*H*)-one derivatives as acetohydroxyacid synthase inhibitors. *J. Agric. Food Chem*. **2006**, *54*, 9135–9139.

(43) Grey, T. L.; Walker, R. H.; Wehtje, G. R.; Adams, J.; Dayan, F. E.; Weete, J. D.; Hancock, H. G.; Kwon, O. Behavior of sulfentrazone in ionic exchange resins, electrophoresis gels, and cation-saturated soils. *Weed Sci*. **2000**, *48*, 239–247.

(44) Dayan, F. E.; Weete, J. D.; Duke, S. O.; Hancock, H. G. Soybean (Glycine max) cultivar differences in response to sulfentrazone. *Weed Sci*. **1997**, *45*, 634–641.

(45) Dayan, F. E.; Weete, J. D.; Hancock, H. G. Physiological basis for differential sensitivity to sulfentrazone by sicklepod (*Senna obtusifolia*) and coffee senna (*Cassia occidentalis*). *Weed Sci*. **1996**, *44*, 12–17.

(46) Li, Z. G.; Wang, Q. M.; Huang, J. M. *Preparation of Organic Intermediates*; Chemical Industry Press: Beijing, China, 1996; p 141.

Received for review July 28, 2009. Revised manuscript received September 12, 2009. Accepted November 19, 2009. We are grateful for financial support from the National Basic Research Program of China (2010CB126103, 2003CB114400), the National Natural Science Foundation of China (No. 20925206 and 20932005), and the Research Fund for the Doctoral Program of Higher Education (No. 20060511003).